LBL-18438
CONF-850107--6

Lawrence Berkeley Laboratory
UNIVERSITY OF CALIFORNIA

EARTH SCIENCES DIVISION

Presented at the 10th Annual Workshop on Geothermal Reservoir Engineering, Stanford University, Stanford, CA, January 22-24, 1985; and to be published in the Proceedings

NONISOTHERMAL INJECTION TESTS IN FRACTURED RESERVOIRS

B.L. Cox and G.S. Bodvarsson

January 1985

DISTRIBUTION OF THIS DOCUMENT IS UNLIMITED

Prepared for the U.S. Department of Energy under Contract DE-AC03-76SF00098

RECEIVED BY OSTI MAR 25 1985

NOT MICROFILM
COVER

LEGAL NOTICE

This book was prepared as an account of work sponsored by an agency of the United States Government. Neither the United States Government nor any agency thereof, nor any of their employees, makes any warranty, express or implied, or assumes any legal liability or responsibility for the accuracy, completeness, or usefulness of any information, apparatus, product, or process disclosed, or represents that its use would not infringe privately owned rights. Reference herein to any specific commercial product, process, or service by trade name, trademark, manufacturer, or otherwise, does not necessarily constitute or imply its endorsement, recommendation, or favoring by the United States Government or any agency thereof. The views and opinions of authors expressed herein do not necessarily state or reflect those of the United States Government or any agency thereof.

Lawrence Berkeley Laboratory is an equal opportunity employer.

DISCLAIMER

This report was prepared as an account of work sponsored by an agency of the United States Government. Neither the United States Government nor any agency Thereof, nor any of their employees, makes any warranty, express or implied, or assumes any legal liability or responsibility for the accuracy, completeness, or usefulness of any information, apparatus, product, or process disclosed, or represents that its use would not infringe privately owned rights. Reference herein to any specific commercial product, process, or service by trade name, trademark, manufacturer, or otherwise does not necessarily constitute or imply its endorsement, recommendation, or favoring by the United States Government or any agency thereof. The views and opinions of authors expressed herein do not necessarily state or reflect those of the United States Government or any agency thereof.

DISCLAIMER

Portions of this document may be illegible in electronic image products. Images are produced from the best available original document.

NONISOTHERMAL INJECTION TESTS IN FRACTURED RESERVOIRS

LBL--18438

DE85 008676

B. L. Cox and G. S. Bodvarsson
Earth Sciences Division
Lawrence Berkeley Laboratory
University of California
Berkeley, California 94720

INTRODUCTION

Pressure transient tests are conducted on geothermal wells in order to obtain data that can be used to calculate the transmissivity (permeability-thickness product) and the skin factor of the well. Various tests can be used to obtain pressure transient data, including pressure drawdown, build-up, injection and falloff tests, and interference tests. Here we are concerned with the analysis of nonisothermal injection and falloff test data. Injection data from pressure transient tests are commonly interpreted using conventional type-curve or graphical analysis, which usually assumes isothermal fluid flow in porous media. In geothermal reservoirs, these tests are complicated by nonisothermal behavior, fractures, and the presence of multiple fluid phases. However, injection and falloff tests are often favored for the analysis of two-phase reservoirs, because they eliminate the need for assuming relative permeabilities for vapor and liquid phases; these factors are unknown at present.

Injection/falloff data are affected by nonisothermal behavior because of variations of temperature-dependent fluid properties (viscosity, density, expansivity, and compressibility). Over a temperature range of 20-300°C, some of these fluid properties can vary by more than an order of magnitude (Figure 1).

Previous studies of nonisothermal pressure transients include those of Tsang and Tsang (1978), who developed an analytical model of the pressure response to nonisothermal injection, and Bodvarsson and Tsang (1980), who studied pressure transients and migration of thermal fronts in fractured reservoirs. Nonisothermal injection tests in two-phase reservoirs have been analyzed by Garg (1978) and O'Sullivan and Pruess (1980).

The basic methodology for the analysis of injection and falloff test data for porous medium reservoirs has been provided by Bodvarsson and Tsang (1980) and Benson and Bodvarsson (1982); methods for evaluating the skin factor have been developed by Benson (1982) and Benson and Bodvarsson (1983). Sigurdsson et al. (1983) developed methods for relating the nonisothermal injectivity index to the isothermal injectivity index.

The present paper extends the analysis of nonisothermal pressure transient data to fractured reservoirs. Two cases are considered: reservoirs with predominantly horizontal fractures and reservoirs with predominantly vertical fractures. Effects of conductive heat transfer between the fractures and the rock matrix are modeled, and the resulting pressure transients evaluated. Thermal conduction tends to retard the movement of the thermal front in the fractures, which significantly affects the pressure transient data. The purpose of the numerical simulation studies is to provide methods for analyzing nonisothermal injection/ falloff data for fractured reservoirs.

APPROACH

In our study, the computer program PT (Pressure-Temperature; Bodvarsson, 1982) was used to simulate pressure transients during nonisothermal injection and falloff tests. The three-dimensional single-phase simulator employs the integrated finite difference method to discretize the medium and formulate the mass and energy transport equations in a liquid saturated porous medium. PT allows for both pressure-dependent and temperature-dependent fluid properties, which are computed internally to within 1% of the true values. The simulator has been validated against many analytic solutions (Bodvarsson, 1982) and field experiments (Buscheck et al., 1983).

A reservoir with predominantly horizontal fractures is modeled employing a radial grid to represent the fracture elements. The grid extends sufficiently far from the well that boundary elements do not affect the results. We assume that the permeability of the rock matrix is much lower than that of the fractures; the fluid mass exchange between the fractures and the rock matrix is therefore negligible. We model conductive heat transfer between the matrix and the fractures using semi-analytic approximations developed by Vinsome and Westerfeld (1980). Their model is based upon the work of Lauwerier (1955), which considered the problem of conductive heat losses during injection. The semi-analytical approach allows us to accurately model the conductive heat transfer without using volume elements for the rock matrix, hence, reducing a two-dimensional

MASTER

DISTRIBUTION OF THIS DOCUMENT IS UNLIMITED

problem to one-dimension. The accuracy of the heat-loss routine has been verified by comparison with Lauwerier's analytical solution (C. H. Lai, personal communication, 1984).

The vertically-fractured reservoir is modeled using a single vertical fracture; cases are studied for a fracture without gravity (single-layer), and with gravity (multi-layered). We again assume that the fracture is infinite in extent, and that the rock matrix is impermeable. Results are obtained both with and without conductive heat transfer with the rock matrix. For all cases, injection of 100°C fluids into a 250°C reservoir is considered. Figure 2 shows the geometries considered for the reservoir systems modeled.

REINJECTION/FALLOFF TESTS IN POROUS MEDIUM RESERVOIRS

In order to evaluate the results of injection tests in fractured reservoirs, we first need to consider earlier results for porous-medium-type reservoirs. Figure 3 shows the semi-log plot of pressure transients from simulated nonisothermal injection into a porous medium with and without a cold spot around the well (Benson and Bodvarsson, 1982). The cold spot can result either from cooling due to drilling or from previous injection. In Figure 3 we see the effects of no cold spot, and of cold spots with radial distances of 1m, 5m, and 10m from the injection well.

In the case where there is no cold spot, the late-time slope (after 1100 sec) is that of the 100°C injection fluid. Therefore the fluid properties (μ,ρ) corresponding to the injected fluid are used to calculate the transmissivity (permeability-thickness product), where

$$kH = \frac{2.303\, q\, \mu}{4\pi\, m\, \rho} \qquad (1)$$

When a cold spot is present, the data initially follow a slope corresponding to the fluid properties of the cold inner region. Later, when the pressure pulse propagates into the hot outer region, the slope changes corresponding to the fluid properties of the hot outer region. At late times, the thermal front starts to move away from the well and the slope changes again to that reflecting the cold fluid properties. For injection periods on the order of a few hours, the pressure transient data will at all times (except for the first few seconds) follow the slope corresponding to the fluid properties of the hot reservoir fluids. Therefore the transmissivity (kH) in Equation (1) should be calculated using the hot fluid properties for μ and ρ.

In the case of falloff following nonisothermal injection into a porous medium reservoir, Bodvarsson and Tsang (1980) Benson and Bodvarsson (1982) found that the fluid properties corresponding to the hot reservoir fluids must be used. After shut-in, immediately following nonisothermal injection, the reservoir behaves like a composite system, with an inner cold region of low fluid mobility and a hot outer region with high fluid mobility. Once the radius of investigation is greater than the size of the cold spot, the slope reflects the fluid properties of the hot reservoir. Analysis of falloff data is therefore for most cases analogous to analysis of injection data with a pre-existing cold spot.

HORIZONTAL FRACTURE CASE

The pressure transients resulting from nonisothermal injection into a horizontal fracture are shown in Figure 4. The pressure transients mentioned above for a porous medium reservoir are included for comparison. The results show that pressure response depends on the value of the thermal conductivity. If there is no heat transfer between the rock matrix and the fractures the solution for the horizontal fracture case is identical to that for a porous medium reservoir ($\lambda = 0$). On the other hand, if the thermal conductivity is very large ($\lambda = \infty$) the thermal front cannot move away from the well and the results are identical to those for isothermal 250°C injection in porous medium reservoirs. The shaded region shown in Figure 4 represents the range of realistic thermal conductivity values. All of our results indicate that it is reasonable to use average fluid properties to calculate kH; other simulation studies have found this to be true over a range of injection and reservoir temperatures (Bodvarsson et al., 1984). Although more accurate results may be obtained using fluid properties which are more strongly weighted towards the cold injected fluid (i.e., the band is slightly closer to the cold slope), the use of average fluid properties is reasonable when one considers the degree of uncertainty in other parameters.

The different slope of the horizontal fracture case can be explained if one considers the velocity of the thermal front moving away from the well. The advancement of the thermal front in porous medium reservoirs (or in horizontal fractures without heat conduction)is given by:

$$r_{tf}^2 = \frac{\rho_w C_w}{\rho_r C_r} \frac{Qt}{\pi H} \qquad (2)$$

Equation (2) shows that the thermal front moves with a velocity proportional to r^2/t. On the other hand, the movement of the thermal front in horizontal fractures is given by (Bodvarsson and Tsang, 1982):

$$r_{tf}^4 = \frac{(\rho_w C_w)^2 Q^2 t}{4.396\, \rho_r\, C_r\, \lambda \pi^2} \qquad (3)$$

Inspection of Equation (3) shows that in this case the velocity of the thermal front is proportional to r^4/t. The thermal conduction between the rock matrix and the fracture is therefore very effective in retarding the advancement of the thermal front.

The skin factor can be calculated using the methods developed in Benson and Bodvarsson (1982), as long as average fluid properties (μ and ρ) are used. However, additional simulations have shown that, when calculating the skin factor, the compressiblity of the in-situ reservoir fluids must be used in all cases.

Horizontal Fracture with a Cold Spot

The pressure transients for nonisothermal injection into a horizontal fracture with a cold spot generally result in 3 slopes, as in the porous medium case. An early time cold slope is followed by a hot slope, but then by an intermediate slope at late time instead of a cold slope. The larger the cold spot, the larger the pressure increase, because of the high viscosity of the cooler fluids. Thus, we see a parallel set of hot slopes for the horizontal fracture case, similar to those observed in the porous medium case (Figure 3).

The early time slope reflecting the properties of the near well cold spot seen for porous medium reservoirs (Fig. 3) may not be seen in the horizontal fracture case (Figure 5), because of the high fracture permeability compared to that of porous medium reservoirs. Comparison of Figures 3 and 5 also shows that the hot slope at intermediate time lasts a much shorter time for the horizontal fracture case than in the porous medium case. The reason is the small fracture aperture compared to the large thickness of porous medium reservoirs. Therefore, one may expect to see the late time slope representing the average fluid properties in injection test data, even though a large initial cold spot is present.

Horizontal Fracture Step-Rate Tests

In many cases, a series of injection/falloff tests with different flow rates (step-rate tests) are conducted instead of single tests (Sigurdsson and Stefansson, 1977; Sigurdsson, 1978). In our study, we simulate the hypothetical step-rate test shown in Figure 6. We start with an 11-day injection at a rate of 0.2 kg/s followed by a 1-day falloff. This is followed by a second injection test at the same rate. The pressure transients and the location of the thermal front (assumed to be the average of the injection and reservoir temperatures) versus time are shown in Figure 6. The pressure transients for the first injection period show the same characteristics as before (Figure 4) with an early-time hot slope followed by an intermediate slope on the semi-log plot.

The falloff data are plotted on a Horner plot (Figure 7). The pressure transients for the falloff in horizontal fractures exhibit a typical composite reservoir behaviour, with an early-time slope corresponding to that of the cold fluids near the well and then a slope corresponding to the hot reservoir fluids at later time. These results are very similar to those obtained by Bodvarsson and Tsang (1980) and Benson and Bodvarsson (1982) for porous medium falloff tests. In the case of fractured reservoirs, however, the duration of the cold water slope is often very short due to high fracture permeability and the rapid heating through heat conduction from the rock matrix.

The second injection step is analyzed using the multi-rate theory of Earlougher (1977) in a manner similar to that of Benson (1982). Figure 8 gives the results on a semi-log plot. It shows an early slope corresponding to the hot fluid properties and then, at later time, a slope corresponding to the average fluid properties. The transition occurs at less than 20 seconds after the start of the second injection step. The results shown in Figure 8 are quite different from those of porous medium reservoirs, where, for most practical purposes, one expects to see the hot slope at late times (although at very late time the cold slope reappears). This difference is because of heating up of the fracture fluids during the falloff period. However, if the test conditions are such that a cold zone of significant radial extent develops and the falloff is of short duration (so that heating of fracture fluids is small), the test results for the second injection step should show primarily the slope corresponding to the hot reservoir fluids.

VERTICAL FRACTURES

Vertical fractures are modeled both with and without gravity. Vertical fractures without gravity are modeled with a one-dimensional geometry, utilizing a single layer of elements which fully penetrates and is penetrated by the well. The heat loss routine described above is used to simulate the thermal conduction between the fractures and the matrix. The vertical fracture models which include gravity have a two-dimensional planar geometry and penetrate the well at either the top or bottom of the fracture. The length of well intersected by the fracture is assumed to be 50 m, while the total height of the fracture is 500 m (see Figure 2). The initial pressure distribution of the gravity models corresponds to a hydrostatic profile. The parameters used for the vertical fracture models are given in Table 1.

In the present work, we are only interested in examining nonisothermal effects during injection into single vertical fractures. No leakage into the rock matrix is allowed, hence, the results obtained are only valid for short test periods or for vertical fractures in very tight formations.

The pressure transient solution for single infinite vertical fracture fully penetrated by a well is given in dimensionless form (Earlougher, 1977) as:

$$P_D = 2\sqrt{\frac{t_D}{\pi}} \qquad (4)$$

where P_D and t_D are dimensionless pressure and time, respectively. In terms of real parameters, Equation (4) becomes:

$$\Delta P = \frac{2Q\mu}{kHb}\sqrt{\frac{kt}{\varphi\mu c_w}} \qquad (5)$$

where H is height of the fracture and b the thickness of the fracture. Inspection of Equation (5) shows that it is not possible to determine the transmissivity ($k_f b$) of the fractures alone, but the cumbersome parameter $k_f b^2 H^2$. Equation (5) shows that it is convenient to determine this parameter using either log-log plots of pressure versus time, or ΔP vs. $\sqrt{t}$.

If the log of the pressure change versus the log of time is used, a half slope will result as shown in Figure 9. The two curves of 100°C and 250°C for isothermal injection are shifted because of the different viscosity values. It is interesting, however, that for all cases with 100°C injection into a 250°C reservoir, the plot falls along the isothermal 250°C curve. For all cases with 250°C injection into a 100°C reservoir, the curve falls on the isothermal 100°C curve. In other words, no matter what the injection temperature or whether or not conductive effects are included, pressure transients for the vertical fracture without gravity follow a curve reflecting the fluid properties of the hot reservoir temperature.

The presence of a 100 m cold spot around the well results in the log-log plot of pressure transients shown in Figure 10. In this case, the data initially follow the curve reflecting the temperature of the cold spot, but after 100 seconds they follow the curve denoting the hot reservoir temperature.

In plots of ΔP versus $\sqrt{t}$, the slope depends upon the fluid viscosity, so that different slopes emerge for these nonisothermal cases. Figure 11 shows a schematic summary of our results plotted as ΔP versus $\sqrt{t}$. For most practical purposes it is probable that conductive heat transfer will effectively retard the advancement of the thermal front in the fracture, so that the effects of the cold spot will be rather small.

Vertical Fracture Case with Gravity

In order to study the effects of gravity on our results we constructed a two-dimensional vertical model of a fracture as shown in Figure 2. We consider four cases: injection into the top of the fracture, both with and without heat conduction, and injection into the bottom of the fracture, both with and without heat conduction. The ratio of the interval open to the well (50 m) and the total fracture height (500 m) is 0.1.

The results obtained are shown in the ΔP vs $\sqrt{t}$ plot in Figure 12. As the figure shows, the effects of gravity are very small. All cases show a slope similar to that of the hot reservoir, with deviations less than 10%. An exception is the rather unrealistic case of no thermal conduction and injection at the bottom. In this case the cold water basically flows along the bottom of the fracture, creating a rather large zone with high viscosity cold fluids. Consequently, the pressure rise is somewhat higher than in the other cases.

Figure 12 also shows some non-linear behavior in the curves at early times. This is due to the partial penetration and shows up more clearly on the log-log plot (Fig. 13). The pressure data fall above the hot reservoir curve because of the resistance caused by the partial penetration. It is interesting to note that the early-time transients due to the partial penetration last for several hundred seconds for this rather high penetration ratio. A more realistic open interval to the well is perhaps 1 m, which would give much longer early transients due to the lower penetration ratio. If a vertical fracture case is suspected, these early transients would be detected because of the lack of a 1/2 slope.

Although the pressure transients for nonisothermal injection into vertical fractures are not significantly affected by gravity or thermal conduction, the temperature distributions of the various models are quite different. This is illustrated in Figure 14 where the location of the thermal front is shown for the two cases of upper and lower injection. After 1×10^6 s (~ 12 days) the thermal front in the case with upper injection has advanced 5.6 m while for the case with lower injection the thermal front has advanced 12.4 m. The thermal front travels much farther in the case with lower injection because the cold water is denser than the reservoir fluids and cannot easily move upwards. In the case with injection at the top of the fracture, the cold water descends rapidly, so that a large surface area for heat conduction develops (Fig. 14). In the case with lower injection, a much smaller surface area for conductive heating results.

DISCUSSION AND SUMMARY

The pressure transients for nonisothermal injection into horizontal fractures plotted on a semilog plot reflect the thermal properties of the reservoir at early times and the average properties at later times. At times after the thermal front has moved past the well, the average fluid properties should be used to calculate the transmissivity and the skin factor. The reason that the late-time slope lies between the cold and hot slopes is that the advance of the thermal front is slowed by conductive heat transfer between the reservoir and the fracture. For reasonable values of thermal conductivity, this is intermediate between the hot and cold slopes. Data obtained during injection into horizontal fractures with cold spots can be analyzed, in most cases, like data from porous medium reservoirs, using the hot slope for computing kH and skin factor.

This is also the case with falloff data. Our simulations for multi-rate injection tests result in an intermediate slope, although for other conditions the hot slope might be present.

The vertical fracture geometry has very different effects on the nonisothermal pressure transients. The log-log plots of pressure change versus time and the linear plot of pressure change versus $\sqrt{t}$ both result in curves which reflect the temperature of the reservoir in all cases. Neither gravity nor thermal conduction significantly change this result. Therefore, the reservoir properties should always be used to calculate reservoir parameters in cases with vertical fractures. The pressure transients reflect the reservoir properties because, for the vertical fracture geometry, pressure change is a function of the distance from the well rather than a function of the log of this distance. Therefore, since pressure change is integrated over a large distance in the fracture, the hot outer part of the fracture has a much greater effect on the pressure transients than does the cold region close to the well. In the horizontal fracture case, where the pressure change is a function of the log of the distance, the region near the well has much more significant effect once the thermal front advances beyond the well.

We find that the elevation of the injection point in vertical fractures greatly affects the migration of the cold water away from the well. If the well intersects the upper portion of the fracture, gravity will help spread the cold water as it descends, causing a large surface area for conductive heating. Thus, if migration of the cold water is a critical consideration when planning injection well locations in vertically fractured reservoirs, our results indicate that it may be preferable to inject into the upper part of the fractures, rather than the lower part.

NOMENCLATURE

b	aperture, m
c	compressibility, Pa^{-1}
C	heat capacity, J/kg °C
H	reservoir thickness, or vertical fracture height, m
k	permeability, m^2
m	absolute value of the slope on a P vs log t plot
P	pressure, Pa
q	mass flow rate, kg/s
Q	volumetric flow rate, m^3/s
r	radius to an observation point, m
r_{tf}	radial distance to the thermal front, m
t	time, s
t_D	dimensionless time
Δ	difference
λ	thermal conductivity, J/s·m·°C
μ	viscosity, Pa s
ρ	density, kg/m^3
ϕ	porosity

Subscripts

D	dimensionless
in	injection
r	rock
res	reservoir
tf	thermal front
w	water
we	well

ACKNOWLEDGEMENT

The authors thank S. Benson for critical review of this manuscript. This work was supported by the Assistant Secretary for Conservation and Renewable Energy, Office of Renewable Energy, Office of Renewable Technology, Division of Geothermal and Hydropower Technologies of the U.S. Department of Energy under Contract DE-AC03-76SF00098.

REFERENCES

Benson, S., 1982. *Interpretation of non-isothermal step-rate injection tests*, Proceedings of the Eighth Workshop of Geothermal Reservoir Engineering, Stanford University, California, pp. 103-109.

Benson, S. M. and Bodvarsson, G. S., 1982. Nonisothermal effects during injection and falloff tests, SPE paper No. 11137, presented at the 57th Annual Meeting of Society of Petroleum Engineers, New Orleans, Louisiana.

Bodvarsson, G. S., 1982. Mathematical modeling of the behavior of geothermal systems under exploitation, Ph.D. thesis, University of California, Berkeley, 348 pp.

Bodvarsson, G. S., Benson, S. M., Sigurdsson, O., Stefansson, V., and Eliasson, E. T., 1984. The Krafla geothermal field, Iceland: 1. Analysis of well test data, Water Resources Research, Vol. 20, No. 11, pp. 1515-1530.

Bodvarsson, G. S. and Tsang, C. F., 1980. Thermal effects in well tests of fractured reservoirs, Proceedings of the Third Invitational Well-Testing Symposium, Berkeley, California, pp. 110-119.

Bodvarsson, G. S. and Tsang, C. F., 1982. Injection and thermal breakthrough in fractured geothermal reservoirs, Journal of Geophysical Research, Vol. 84, No. B2, pp. 1031-1048.

Buscheck, T. A., Doughty, C. and Tsang, C. F., 1983. Prediction and analysis of a field experiment on a multilayered aquifer thermal energy storage system with strong buoyancy flow, Water Resources Research, Vol. 19, No. 5, pp. 1307-1315.

Earlougher, Jr., R. C., 1977. Advances in well test analysis, Society of Petroleum Engineers, Monograph 5.

Lauwerier, H. A., 1955. The transport of heat in an oil layer caused by injection of hot fluid, App. Sci. Research, Sec. A., Vol. 5, pp. 145-151.

O'Sullivan, M. J. and Pruess, K., 1980. Analysis of injection testing of geothermal reservoirs, Geothermal Resources Council Transactions, Vol. 4, pp. 401-404.

Pruess, K. and Bodvarsson, G. S., 1983. Thermal effects of reinjection in geothermal reservoirs with major vertical fractures, SPE paper No. 12099.

Sigurdsson, O., 1978. Rennsliseiginleikar efra jardhitakersins. Kraflu, OS/JHD-7851, report in Icelandic, National Energy Authority, Reykjavik, Iceland.

Sigurdsson, O. and Stefansson, V., 1977. Lekt i borholum i Kroflu, OS/JHD-7727 report in Icelandic, National Energy Authority, Reykjavik, Iceland.

Tsang, Y. W. and Tsang, C. F., 1978. An analytic study of geothermal reservoir pressure response to cold water reinjection, Proceedings Fourth Workshop on Geothermal Reservoir Engineering, Stanford University, California, pp. 322-331.

Vinsome, P. K. W. and Westerveld, J., 1980. A simple method for predicting cap and base rock heat losses in thermal reservoir simulations, J. Canadian Petrol Tech., July-Sept., pp. 84-90.

Table 1. Parameters used in Simulations

	Horizontal Fracture	Vertical Fracture - no Gravity	Vertical Fracture with Gravity
K_f	2×10^{-11} m^2	2×10^{-11} m^2	1×10^{-8} m^2
K_r	0	0	0
b	.01 m	.01 m	.01 m
ϕ_f	.999	.999	.999
q	.2 kg/s	2×10^{-5} kg/s	2 kg/s
r_{we}	.1 m	.1 m	5 m
λ_r	2.0 J/m s°C	2.0 J/m s °C	2.0 J/m s °C
e_r	2650 kg/m^3	2650 kg/m^3	2650 kg/m^3
$c_{r_{rock}}$	1000 J/kg°C	1000 J/kg°C	1000 J/kg°C
H	-	1 m	500 m
T_{res}	250°C	250°C	250°C
T_{in}	100°C	100°C	100°C

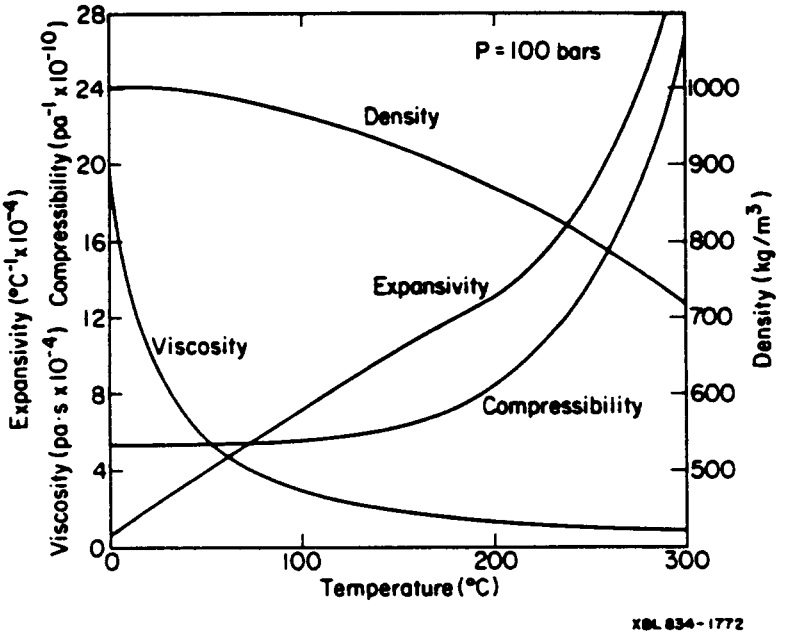

Figure 1. Variations in fluid properties of liquid water with temperature (from Bodvarsson et al., 1984).

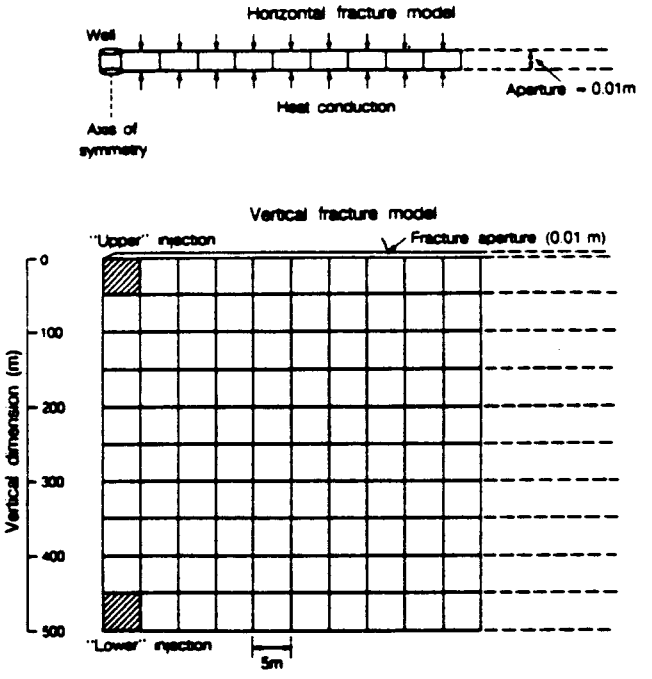

Figure 2. Horizontal and vertical fracture model geometries.

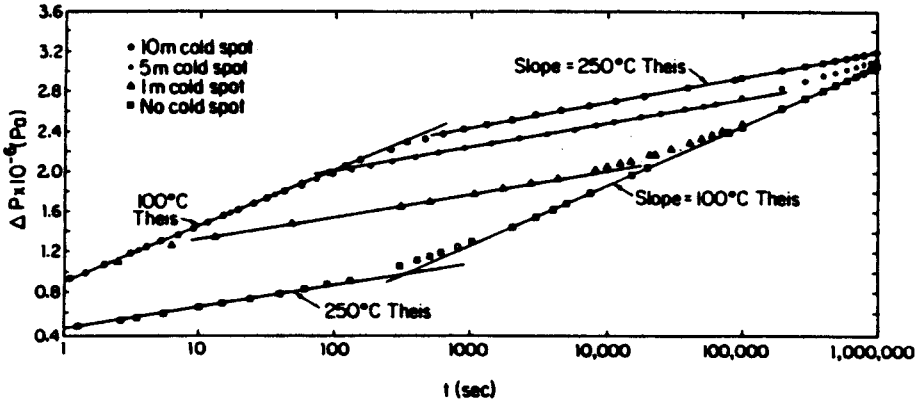

Figure 3. Pressure transient data from 100°C injection into a 250°C porous medium reservoir with a cold spot (after Benson and Bodvarsson, 1982).

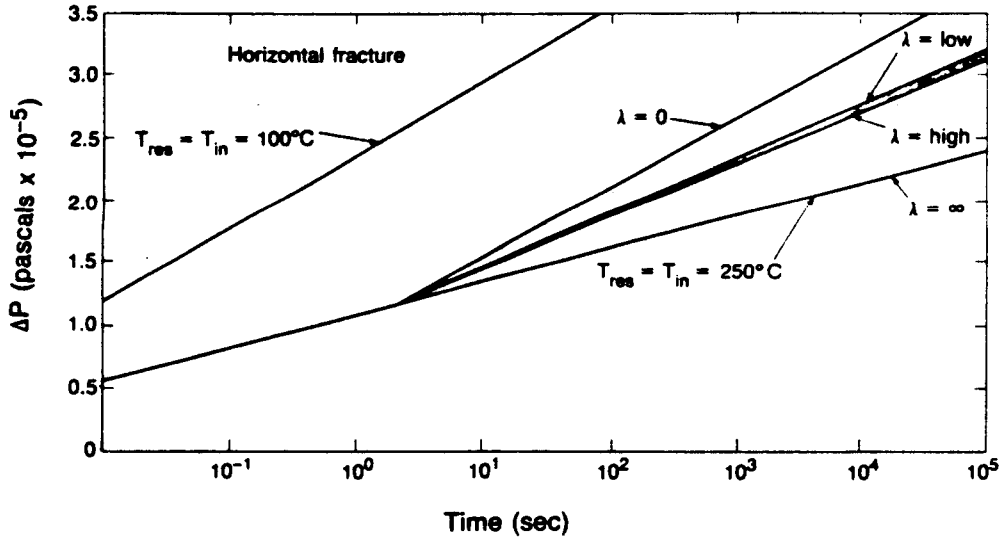

Figure 4. Pressure transient data for nonisothermal injection into a horizontal fracture.

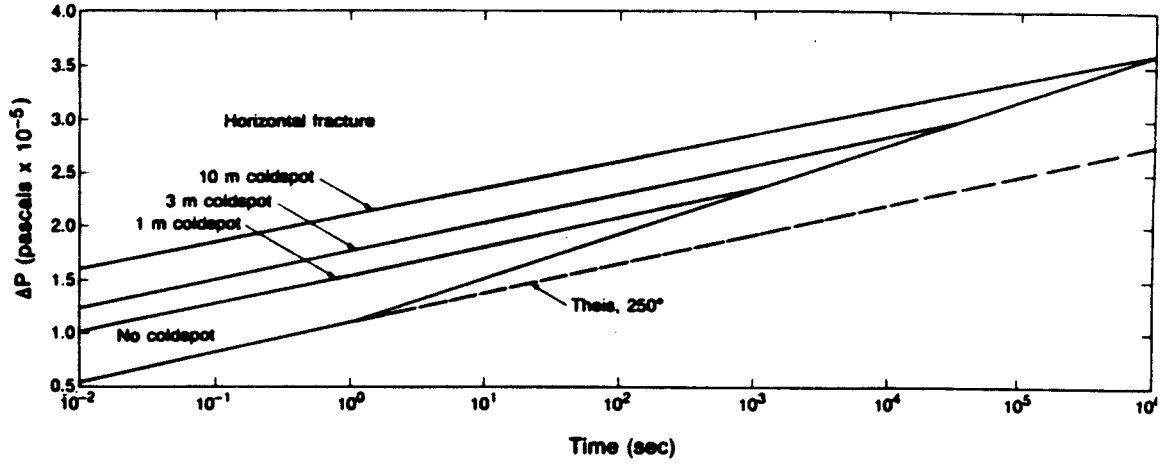

Figure 5. Pressure transients for non-isothermal injection into a horizontal fracture with cold spots.

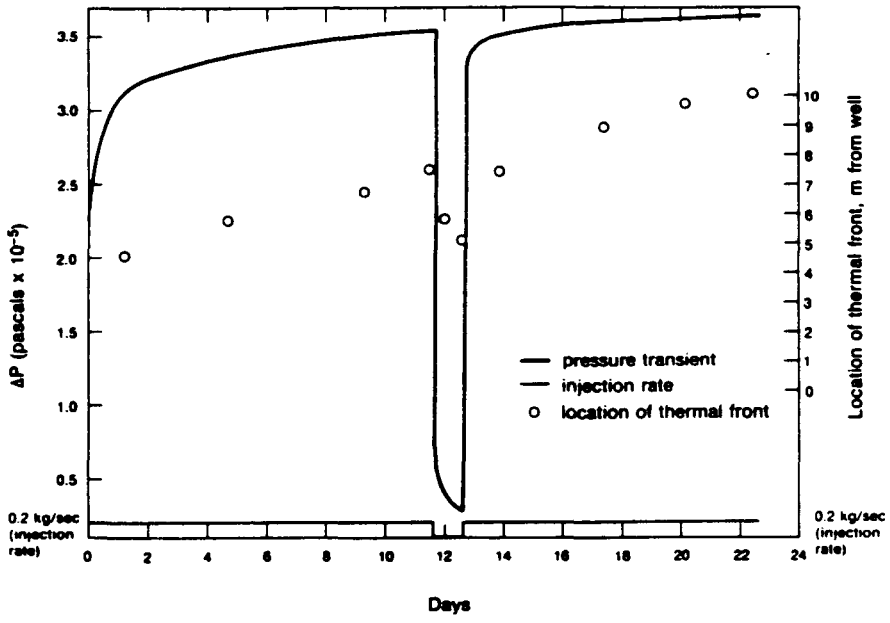

Figure 6. Step-rate non-isothermal injection test data for a horizontal fracture.

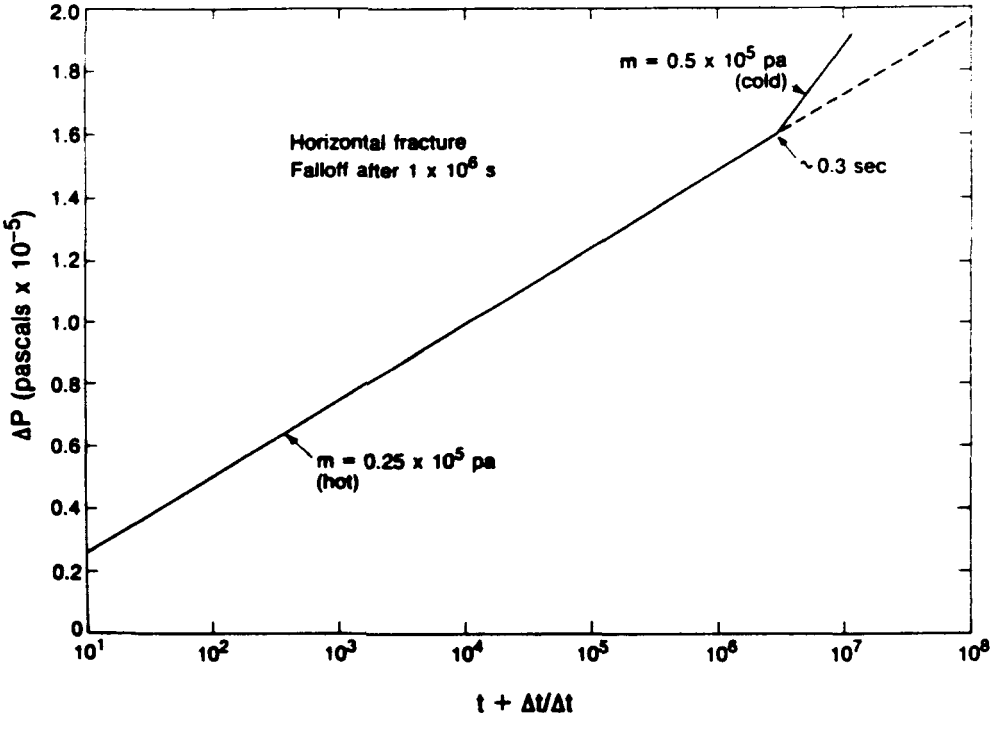

Figure 7. Pressure transient data for falloff after 10^6 (f 11days) of 100°C injection into a 250°C horizontal fracture.

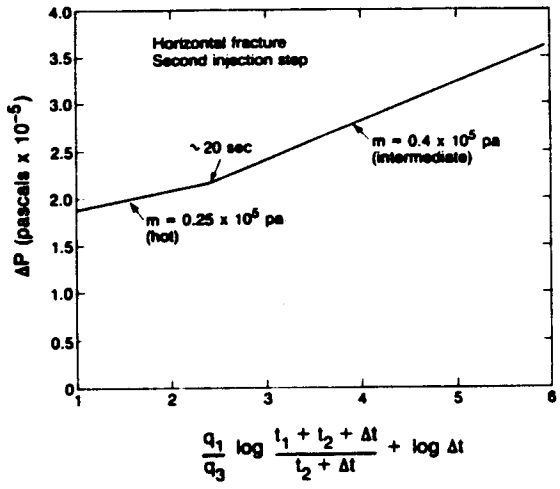

Figure 8. Multi-rate analysis of the pressure transient data for the second injection step in a horizontal fracture.

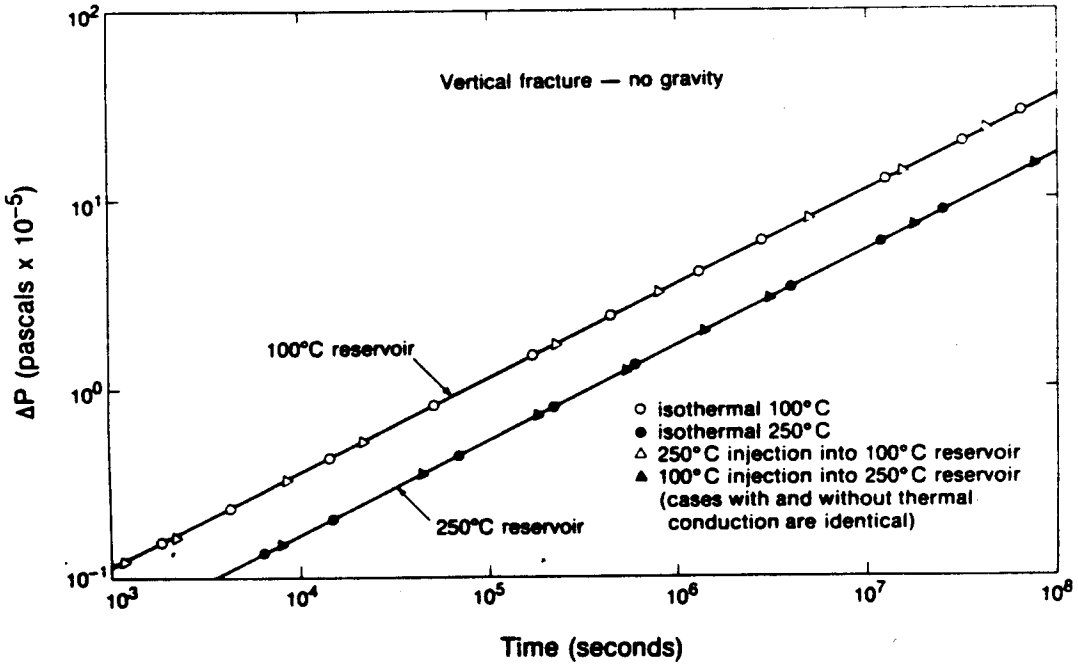

Figure 9. Pressure transients (log-log) for non-isothermal injection into a vertical fracture (no gravity).

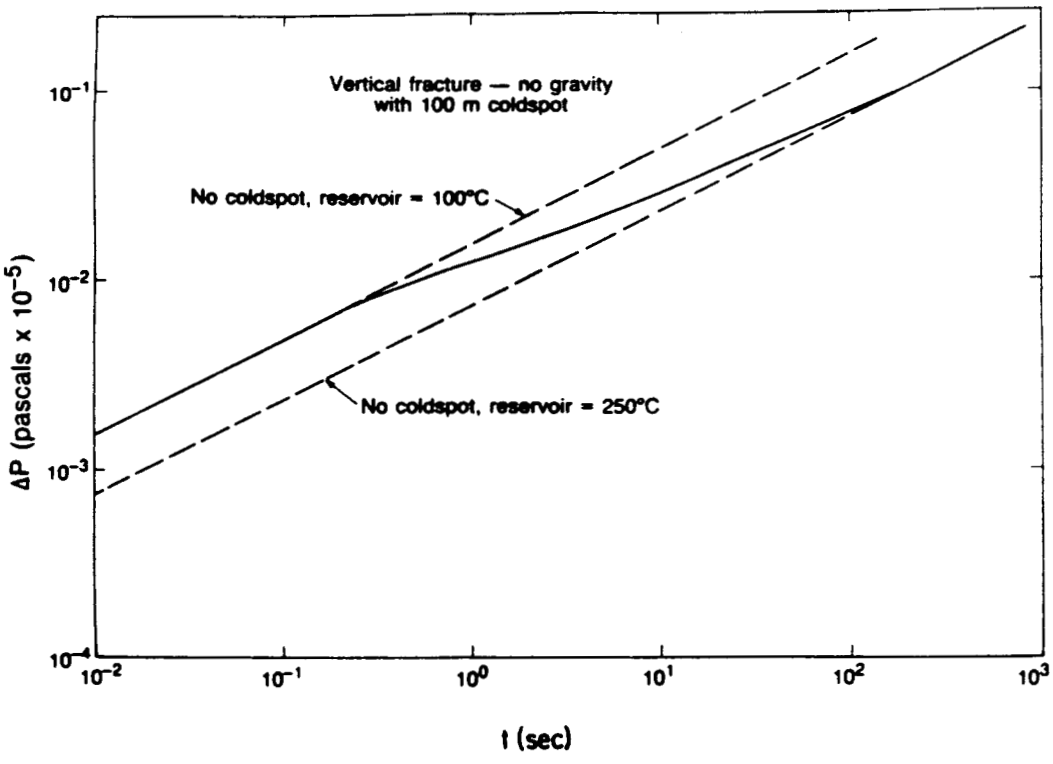

Figure 10. Pressure transients (log-log) for non-isothermal injection into a vertical fracture (no gravity) with a cold spot.

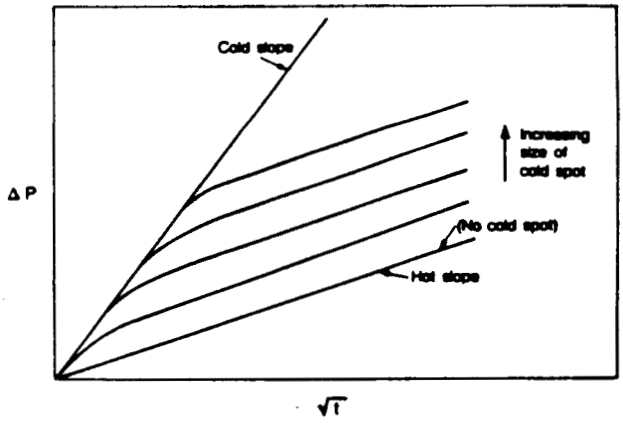

Figure 11. Schematic pressure transients (ΔP vs $\sqrt{t}$) for non-isothermal injection into a vertical fracture (no gravity) with cold spots.

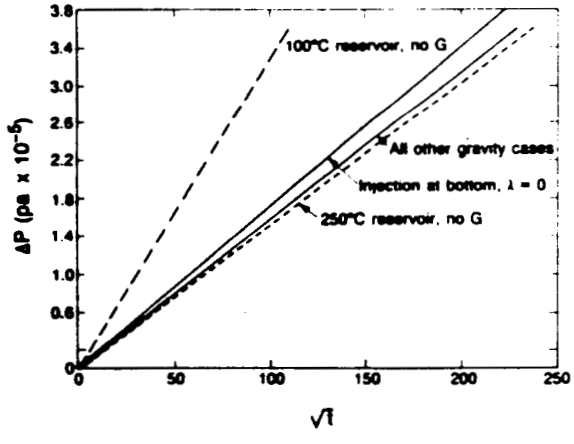

Figure 12. Pressure transients (ΔP vs $\sqrt{t}$) for non-isothermal injection into a vertical fracture with gravity.

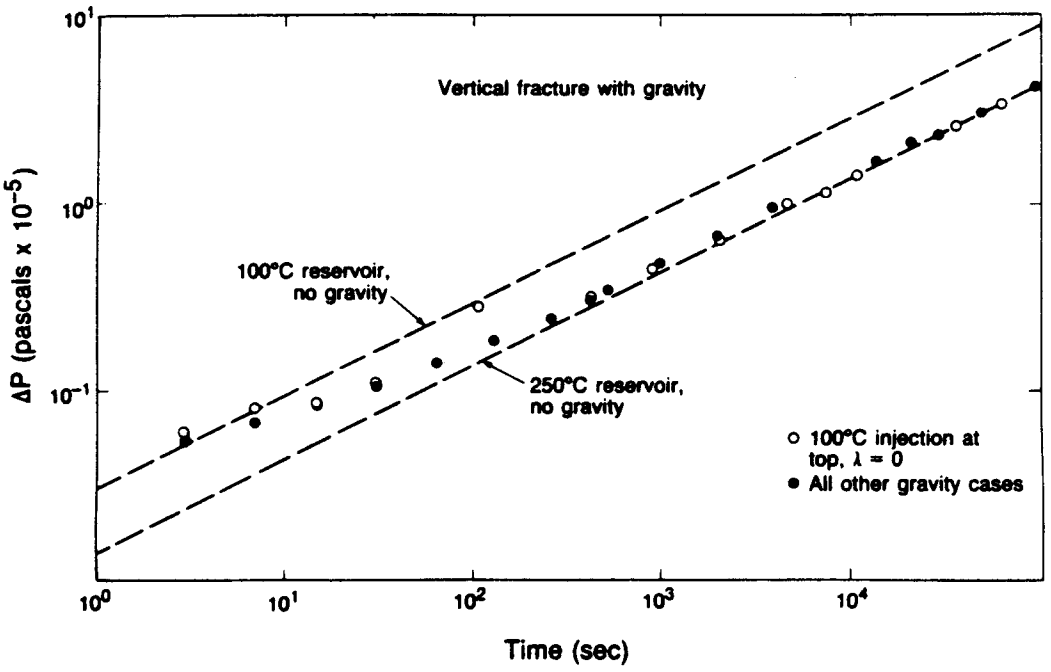

Figure 13. Pressure transients (log-log) for non-isothermal injection into a vertical fracture with gravity.

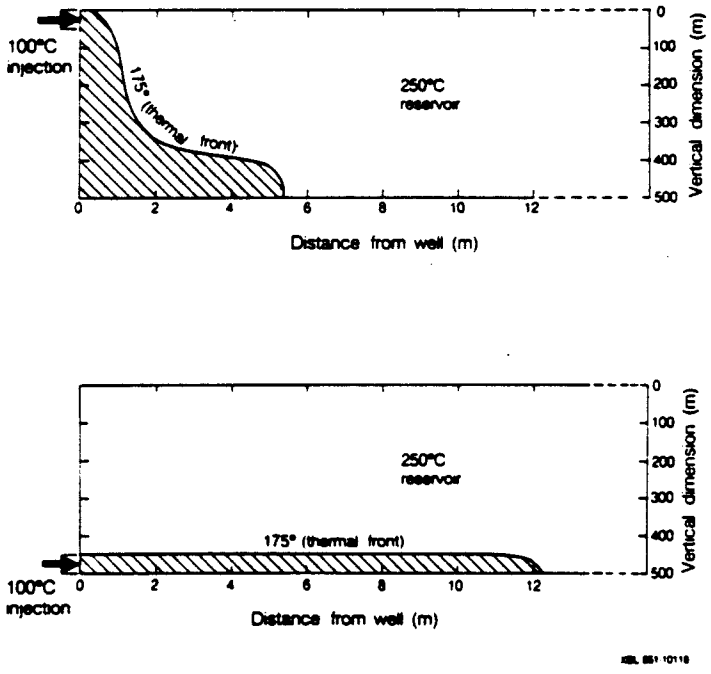

Figure 14. Schematic view of thermal front for non-isothermal injection into a vertical fracture for cases of upper injection and lower injection.